Renewable and Sustainable Energy Reviews 37 (2014) 585–598

Contents lists available at ScienceDirect

Renewable and Sustainable Energy Reviews

journal homepage: www.elsevier.com/locate/rser

# A comprehensive review of maximum power point tracking algorithms for photovoltaic systems

Nur Atharah Kamarzaman [a], Chee Wei Tan [b,*]

[a] Department of Electrical Engineering, Faculty of Electrical Engineering, Universiti Teknologi Mara, Pulau Pinang, Malaysia
[b] Department of Electrical Power Engineering, Faculty of Electrical Engineering, Universiti Teknologi Malaysia, Skudai, Malaysia

ARTICLE INFO

*Article history:*
Received 22 March 2013
Received in revised form
5 May 2014
Accepted 17 May 2014

*Keywords:*
Maximum power point tracking (MPPT)
Photovoltaic (PV) systems
Partial shaded
Uniform solar irradiance

ABSTRACT

In recent decades, Photovoltaic (PV) energy has made significant progress towards meeting the continuously increasing world energy demand. Besides that, the issue of conventional fossil fuels depletion as well as environmental pollution both contribute to the growth of PV technology. However, the deployment and implementation of photovoltaic systems remain as a great challenge, since the PV material cost is still very high. The low PV module conversion efficiency is another factor that restricts the wide usage of PV systems, therefore a power converter embedded with the capability of maximum power point tracking (MPPT) integrated with PV systems is essential to further the technology. This paper provides a comprehensive review of the available MPPT techniques, both the uniform insolation and partial shaded conditions. In order to appreciate the knowledge of MPPT concepts, several types of PV cell equivalent models are explained too. Conventional MPPT techniques have proven the ability to track the maximum power point (MPP) under uniform solar irradiance. However, under rapidly changing environments and partially shaded conditions, conventional techniques have failed to track the true MPP. For this reason, stochastic based methods and artificial intelligence have been developed with the ability to seek the true MPP under multiple peaks with good convergence speed. This paper analyses and compares both conventional and stochastic MPPT techniques based on the true MPP tracking capability, design complexity, cost consideration, sensitivity to environmental change and convergence speed. Comparatively, the stochastic algorithms and artificial intelligence show excellent tracking performance. The research on MPPT techniques is ongoing towards achieving a better performance in terms of the ease of implementation, low system cost and better tracking efficiency.


**Contents**

1. Introduction . . . 586
2. Photovoltaic characteristics . . . 586
3. The effect of partial shading . . . 588
4. Maximum power point tracking . . . 588
   4.1. Conventional MPPT Algorithms . . . 589
      4.1.1. Perturb and observation . . . 589
      4.1.2. Incremental conductance . . . 589
   4.2. Hill climbing . . . 590
      4.2.1. Open-circuit voltage and short-circuit current . . . 590
   4.3. Ripple correlation current . . . 591
   4.4. Stochastic based MPPT algorithms . . . 591
      4.4.1. Particle swarm optimization . . . 591
      4.4.2. Fuzzy logic controller . . . 592
      4.4.3. Artificial neural network . . . 593
      4.4.4. Differential evolution . . . 594

* Corresponding author.
*E-mail addresses:* cheewei@fke.utm.my, dr.c.w.tan@gmail.com (C.W. Tan).

http://dx.doi.org/10.1016/j.rser.2014.05.045
1364-0321/

4.4.5. Initialization . . . 594
4.4.6. Mutation. . . . 594
4.4.7. Crossover . . . 594
4.4.8. Evaluation and selection . . . 594
5. Genetic algorithm . . . 595
6. Discussions. . . . 595
6.1. Design complexity . . . 596
6.2. Ability to track the true MPP . . . 596
6.3. Cost consideration . . . 596
6.4. Sensitivity . . . 596
6.5. Convergence speed . . . 596
7. Conclusion . . . 596
References . . . 597

## 1. Introduction

Up to date, the photovoltaic (PV) power generation has shown a significant potential in fulfilling the growing world's energy demand. Up to the year 2011, global operation of solar power generation has risen up to 70 $GW_p$, in which almost 30 $GW_p$ solar power came into the market in 2011 [1,2]. In year 2012, the total PV operating capacity has increased to 100 $GW_p$ [3]. Solar energy has gained much popularity as it is a form of renewable energy with many advantages. In Malaysia, sunshine is available throughout the year. Solar energy offers no fuels costs, no pollution and needs little maintenance. There are many applications of PV system that have been developed and reported [4,5]. However, the deployment and implementation of photovoltaic systems still remains a great challenge due to the very high initial investment cost. It is not only the cost of PV array that needs to be considered, but also the cost of equipment for energy conversion that should be taken into account. This means that the energy produced by PV is relatively high as compared to conventional energy production. Furthermore, there is no guarantee that the energy produced from PV array keeps constant, because it depends entirely on the solar irradiance and the ambient temperature. Second, the energy produced by the sun is restricted by the low PV module conversion efficiency. In short, a power converter embedded with the capability of maximum power point tracking (MPPT) is essential in all PV systems to ensure the best energy harvesting from the prevailing environmental conditions.

There have been many studies made on MPPT techniques. For instance, the perturb and observation (P&O) [6–22] and the hill climbing (H&C) [6,23–30] technique are widely used as MPPT due to the simple implementation and also fewer sensor requirements. The incremental conductance (IncCond) algorithm [31–41], which compares incremental and instantaneous conductance of PV arrays, is able to track the maximum power point of a PV system and transfer high PV energy to the load. Ripple correlation control (RCC) [42–44] has introduced ripple into the control strategy by the aid of switching the converter to control the MPPT. This technique performs well at high solar irradiance but the tracking efficiency drops at low sun irradiance. Alternatively, by shedding the load of the PV array, the current and voltage at the maximum power point (MPP), $I_{\text{MPP}}$ and $V_{\text{MPP}}$, of the PV system can be determined by short-circuit current, $I_{SC}$ [45–48] and open-circuit voltage, $V_{OC}$ [49–55] techniques. However, the main drawback of this MPPT is the uncertainty which exists in this tracking method as shown by the approximate relationship of $I_{SC}$ to $I_{\text{MPP}}$ and $V_{OC}$ to $V_{\text{MPP}}$.

In recent years, further research on PV MPPT has been conducted and the effect of partial shading has been taken into account. Researchers have found that the conventional methods show very poor tracking performance and many of them are not even able to track the true MPP under partially shaded PV array. Due to the drawbacks of conventional MPPT algorithms, several stochastic-based algorithms and artificial intelligence techniques have been developed. These new MPPT algorithms, inspired by nature and biological structure, have been developed to maximize output power from PV array. They include: particle swarm optimization (PSO) [56–61], differential evolution (DE) [62], genetic algorithm (GA) [63] and artificial neural network (ANN) [59,64–66]. Besides that, the fuzzy logic controller (FLC) [66–72], which is based on the logical interpretation of data, can find the solution to extract the maximum power under partially shaded and rapidly varying atmospheric condition. To date, there are many research papers which have discussed and compared the operation of each of MPPT technique. Nevertheless, the literature reviews are not up to date and do not cover all available MPPT techniques for both uniform and partial shaded conditions. Thus, this paper is written to review the available MPPT techniques comprehensively, include both uniform and partial shaded conditions.

This paper is organized as follow, where the next section describes the brief concept of four PV cell models. The next section provides an overview of the characteristic of partial shading followed by explanation of the MPPT techniques. The MPPT techniques are divided into two categories: the conventional method for uniform solar irradiance, and the stochastic-based algorithm and artificial intelligence techniques for partial shading conditions. Finally, comparison and discussion on the characteristics of MPPT techniques are clarified and conclusions are drawn.

## 2. Photovoltaic characteristics

Photovoltaic originates from two separate words- *photo*, which means light, and *voltaic*, that refers to the generation of electricity [73]. Therefore, 'photovoltaic' brings the meaning of producing electricity directly from the sun. Solar arrays consist of several combinations of solar modules, where each module is made up from a number of solar cells. It is noted that solar cells are made from layers of semiconductor material, which are commonly made from crystal silicon [73].

From the literature, there are few types of equivalent circuit models to represent PV cells. A well-known circuit model is the generic model which has single diode with a series resistance and a shunt resistance [74,75]. As shown in Fig. 1, the amount of electrical energy produced by PV is represented by the current $I_{ph}$, which is proportional to the solar irradiation. The series resistor represents an internal resistance while the shunt resistance represents the leakage current.

The mathematical equation that expresses the PV cell is given in as follows:

$$I_{\text{PV}} = I_{Ph} - I_D - \frac{V_D}{R_{sh}} \tag{1}$$

The diode characteristic is expressed by

$$I_D = I_0\,(e^{V_D/V_T A} - 1) \tag{2}$$

The diode voltage is expressed by

$$V_D = (V_{PV} + I_{PV} R_s) \tag{3}$$

Photocurrent $I_{Ph}$ is given by

$$I_{Ph} = (I_{SC} + K_1(T - T_{Ref}))\lambda \tag{4}$$

The variables are defined as follows

$I_0$ is the cell saturation of dark current, $V_T$ is the thermal voltage of PV modules which is equal to $kT/q$, $q$ is the electron charge ($1.6 \times 10^{-19}$ C), $k$ is the Boltzman constant which is equal to $1.38 \times 10^{-23}$ J/K, $T$ is the temperature of p–n junction in unit Kelvin, $A$ is the diode ideality factors which depend on the PV technology, $I_{SC}$ is the cell's short- circuit current at standard test condition (1000 W/m$^2$ and 25 °C), $K_1$ is the coefficient of the cell's short-circuit current, $T_{Ref}$ is the cell's reference temperature, $\lambda$ represents the solar irradiance in unit W/m$^2$.

Another PV model which is more accurate to describe PV cell behaviour is the two-diode model [76,77] as shown in Fig. 2. The two-diode model consists of the photocurrent, two parallel diodes, a shunt resistor and a series resistor. The mathematical expression of this model is given by

$$I_{PV} = I_{ph} - I_{D1} - I_{D2} - \frac{V_D}{R_{sh}} \tag{5}$$

where

$$I_{D1} = I_{01}(e^{V_D/V_T A_1} - 1) \tag{6}$$

and

$$I_{D2} = I_{02}(e^{V_D/V_T A_2} - 1) \tag{7}$$

while $V_{Diode1} = V_{Diode2} = V_D$. The variables, $A_1$ and $A_2$ are the diode ideality factors, which depend on the PV technology, for diode 1 and diode 2, respectively.

The two-diode PV cell model, however, requires more parameters to be considered than the single diode model. Moreover, due to the implicit and non-linear behaviour of the PV model, the model is rarely used. Recently, Ishaque et al. [78] have introduced a simple and fast two-diode photovoltaic model that able to reduce the computational time, as shown in Fig. 3. The model can be expressed as

$$I_{PV} = I_{Ph} - I_0\,(I_p + 2) - \frac{V_D}{R_{sh}} \tag{8}$$

where

$$I_{Ph} = (e^{V_D/V_T} + e^{V_D/(P-1)V_T}) \tag{9}$$

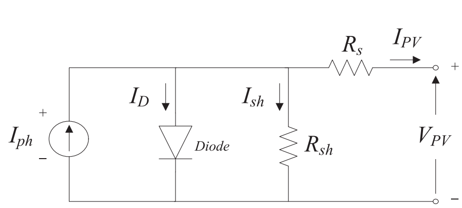


**Fig. 1.** The single diode model of PV cell.

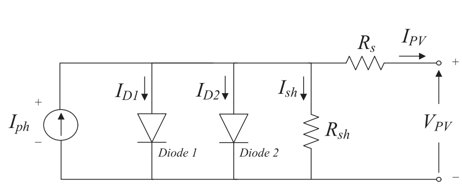


**Fig. 2.** The two-diode model of PV cell.

and

$$p = 1 + A_2$$

since

$$(A_1 + A_2)/p = 1 \text{ and } A_1 = 1 \tag{10}$$

where $A_1$ and $A_2$ are the diode ideality factor for diode 1 and diode 2, respectively.

The shunt resistance, $R_{sh}$, can be represented as an open-circuit because its value is too large as compared to the series resistance [76], as shown in Fig. 3. Therefore, the variation of the $R_{sh}$ brings negligible impact on the PV model output; however even a small variation of the $R_s$ would affect the PV efficiency. The mathematical expression is given by:

$$I_{PV} = I_{Ph} - I_D \tag{11}$$

and $I_D$ refers to (2)

When considering the ideal PV cell, the series' losses are zero ($R_s = 0$) and the leakage to ground is negligible, $R_{sh} = \infty$, hence the effect of these two parameters can be neglected. Mathematical expression in (1) is rewritten to express simplified model in Fig. 4.

$$I_{PV} = I_{Ph} - I_0\left(e^{V_{PV}/V_T A} - 1\right) \tag{12}$$

Figs. 5 and 6 show the $P$–$V$ and $I$–$V$ characteristics of a generic PV array. Both characteristics show that the output of PV array is non-linear, which governed by the solar irradiance. Under the condition of full illumination, there is only one peak on the $P$–$V$ characteristic. However, when partial shading occurs, the PV characteristics change so that multiple peaks exist.

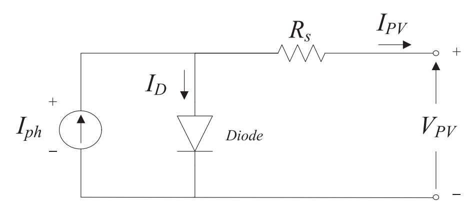


**Fig. 3.** The single diode model of PV cell without shunt resistance.

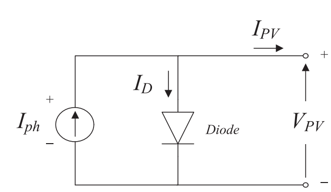


**Fig. 4.** The simplified model of PV cell without series and shunt resistance.

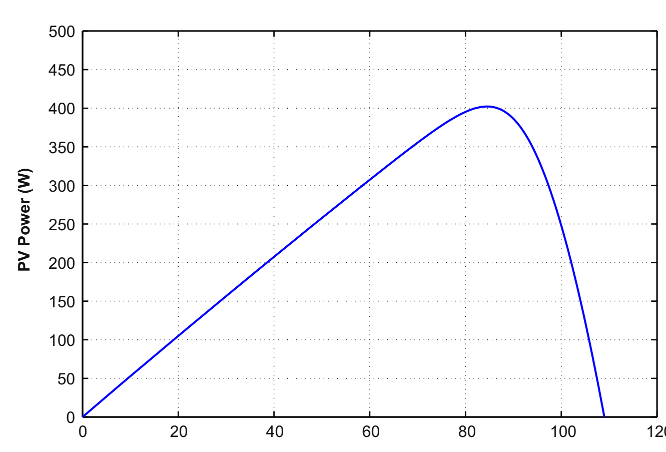


**Fig. 5.** The $P$–$V$ characteristic of a typical PV array.

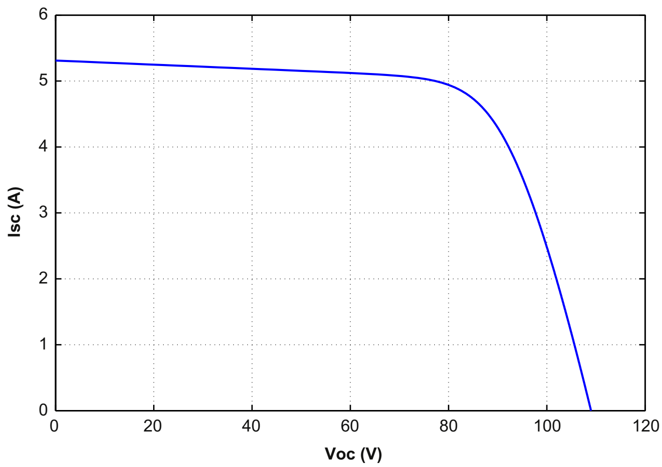


**Fig. 6.** The *I–V* Characteristic of a typical PV array.

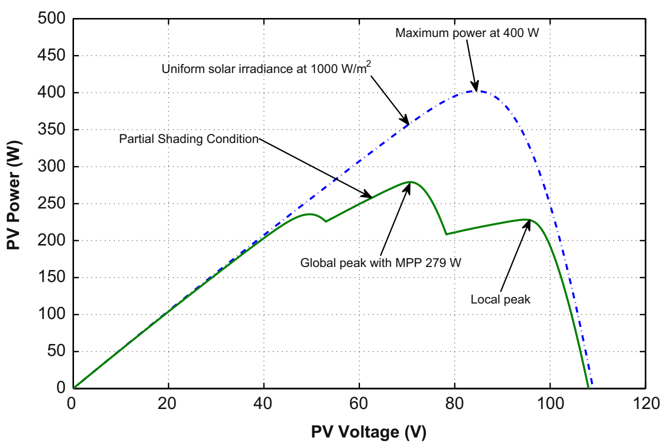


**Fig. 7.** A comparison of the *P–V* characteristics between uniform solar irradiance and partial shading condition.

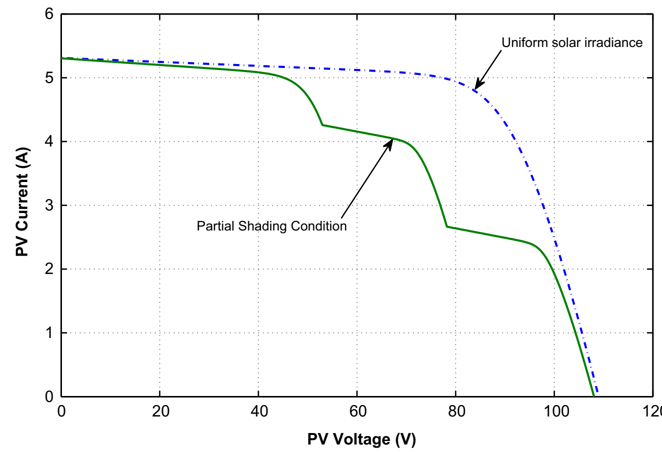


**Fig. 8.** A comparison of the *I–V* characteristic between uniform solar irradiance and partial shading condition.

## 3. The effect of partial shading

In PV systems, the PV output power generated depends on solar irradiance and the ambient temperature. These two factors determine the true Maximum Power Point (MPP). In general, temperature influences the PV output voltage while solar irradiance affects PV output current [79]. In other word, when PV array receives high solar irradiance, the output current is high, and vice versa. Based on the *I–V* and *P–V* characteristic curves, there is only one optimum point which delivers the maximum power to the system.

Due to the non-linear characteristic of PV array, the energy produced from PV array is not constant. In any case, where some parts of PV array are shaded by a nearby tree, chimney, or cloud, partial shading condition would occur. Under partial shading conditions, the shaded region of PV receives less intensity of sunlight as compared to other region. The shaded PV module would absorb a large amount of the electric power that is generated by the non-shaded PV modules. This scenario is called the hot spot problem, and can damage PV cells [62,66,70]. To overcome this, a bypass diode is commonly connected in parallel with each PV module in order to provide an alternative path during partial shading, helping to avoid damage of PV module. Nevertheless, the insertion of a bypass diode causes the existence of multiple peaks on the *P–V* and *I–V* characteristics. Fig. 7 and Fig. 8 show the characteristics of PV under the uniform solar irradiance and partial shading condition.

Referring to Figs. 7 and 8, it can be observed that the *P–V* characteristics consist of multiple peaks and the *I–V* characteristic has multiple steps due to partial shading. Among the multiple peaks, there is only one global peak (GP), which is the true MPP, while others are the local peaks (LP).

## 4. Maximum power point tracking

Based on the *I–V* curve, it can be seen that the PV operating point may vary from zero to the open-circuit voltage. The operating point does not always stay at the maximum power point but varies with load. Therefore, the system does not always supply the fullest available solar energy to the load. A very simple approach can be taken to solve this problem by increasing numbers of PV modules in the system, which is more than the required capacity. Nevertheless, this will increase the system cost and energy losses [80]. In order to solve this problem, a revolutionary type of power electronic device, MPPT, is introduced to determine the maximum operating point. A PV system that connects to an MPPT controller is able to search for the MPP and make best use of the PV array. With that, the PV system is assured to continuously operate at the true MPP [80].

Various MPPT algorithms have been developed for PV systems. These can be categorised into conventional techniques and recent development which are based on stochastic technique. The former technique has been developed and shows good performance to track the MPP under uniform solar irradiance. However, under rapidly changing environment and partial shading condition, the conventional MPPT algorithms failed to track the global peak. Hence, stochastic based and artificial intelligence methods have been developed to extract the optimum power from a PV system under any atmospheric condition, including partial shading. The important criterion when choosing an algorithm is the capability of it to track the true MPP among the local peaks with cost and convergence speed considered. The list of MPPT algorithms is shown in Table 1.

In this paper, the presentation of the MPPT algorithms is organized into two categories. In the first part, the conventional MPPT algorithms which can work satisfactorily under uniform solar irradiance are discussed. In the second part, the MPPT algorithms based on stochastic algorithms which can work satisfactorily under both uniform sun irradiance and partial shading are explained.

**Table 1**
The MPPT algorithms under uniform and partial shading condition.

| MPPT algorithms | |
|---|---|
| Uniform irradiance condition | Partial shading condition |
| a. Perturb and observation | a. Particle swarm optimization |
| b. Hill Climbing | b. Genetic algorithm |
| c. Incremental conductance | c. Differential evolution |
| d. Fractional voc | d. Artificial neural etwork |
| e. Fractional Isc | e. Fuzzy logic controller |
| f. Ripple correlation control | |
| g. Current sweep | |
| h. DC link capacitor droop control | |
| i. Load current or load voltage maximization | |
| j. *dP/dV* or *dP/dI* feedback control. | |

### 4.1. Conventional MPPT Algorithms

#### 4.1.1. Perturb and observation

The application of the perturb and observation (P&O) algorithm has been widely used due to ease of implementation. Initially, the present value of the PV voltage and the PV current are sensed to obtain the PV power. In the P&O algorithm, the voltage of the PV array output is perturbed by a small increment which results in a change of power, $\Delta P$. If the $\Delta P$ is positive, the perturbation will move the operating voltage toward the MPP. Then, the perturbation size ($C$), is generated in the same direction. In case of a negative $\Delta P$, the system is operated far from the optimal point, thus the perturbation size needs to be reduced in order to bring the operating point back to the MPP [19,80–82]. The flow chart of the P&O MPPT algorithm is presented in Fig. 9.

Based on the flow chart, when the instantaneous PV power increases with the operating voltage, the operating point is moving towards the MPP. This means the perturbation size is positive or remains unchanged. When the instantaneous PV power reduces while the operating voltage also reduces, the operating point is moving away from the MPP. Therefore, the perturbation size is reverted to force the operating point back to the true MPP. The drawback of this algorithm is that the tracking efficiency reduces under rapidly environmental change. The MPPT is not able to determine the actual maximum point. It oscillates around the MPP continuously and changes the sign of perturbation after measurement of $\Delta P$. Besides that, in the case of varying solar irradiance, the P&O fails to determine the true MPP [82].

#### 4.1.2. Incremental conductance

The incremental conductance MPPT algorithm is based on the $dP/dV$, which equals to zero at the point of the MPP. Referring to Fig. 10, the gradient at the MPP point is zero, correspondingly, a positive gradient on the left of the MPP and a negative gradient on the right of the MPP. The power gradients can be summarized as

$$\begin{aligned} &dP/dV = 0 \quad \text{at MPP} \\ &dP/dV > 0 \quad \text{left of MPP} \\ &dP/dV < 0 \quad \text{right of MPP} \end{aligned}$$

From the $I$–$V$ and $P$–$V$ characteristics,

$$\frac{dP}{dV} = \frac{d(IV)}{dV} = I + V\frac{dI}{dV} \cong V\frac{\Delta I}{\Delta V} \tag{13}$$

Thus, the point of $dP/dV$ can be written as

$$\begin{aligned} &(\Delta I/\Delta V) = -I/V, \quad \text{at MPP} \\ &(\Delta I/\Delta V) > -I/V, \quad \text{left of MPP} \\ &(\Delta I/\Delta V) < -I/V, \quad \text{right of MPP} \end{aligned}$$

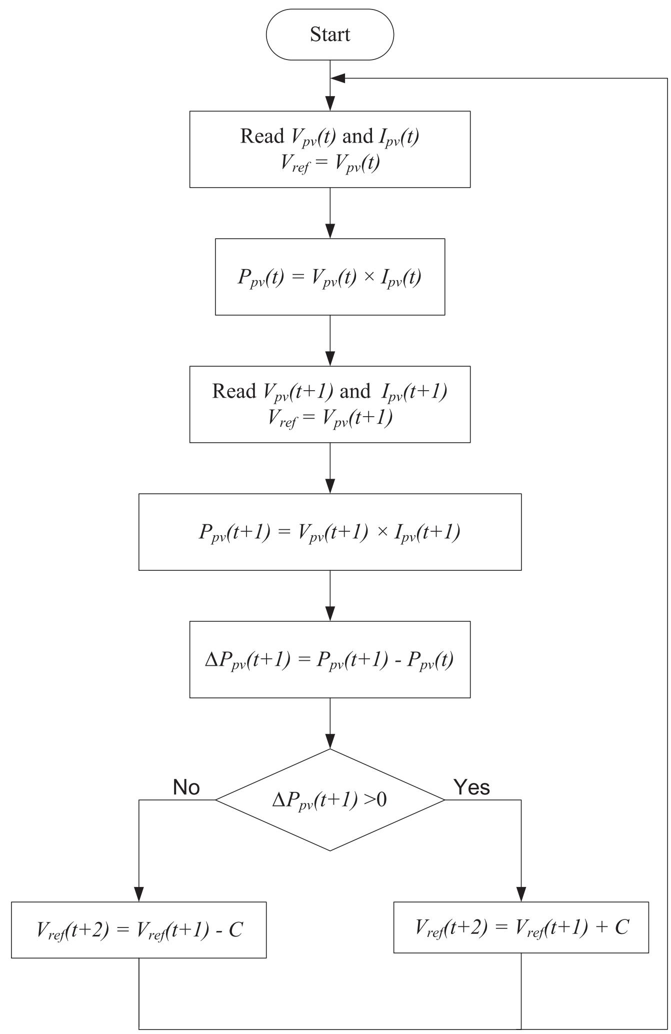


**Fig. 9.** The flow chart of perturb and observe MPPT algorithm.

The IncCond algorithm starts the cycle by obtaining current value of $V$ and $I$ at $V(t)$ and $I(t)$. Based on the flow chart as shown in Fig. 11, MPP can be tracked by comparing instantaneous conductance ($I/V$) to the incremental conductance ($\Delta I/\Delta V$). Control signal voltage, $V_{\text{ref}}$, is adjusted too- it needs to be decreased or increased based on output of the comparison above. The MPP is reached once the $V_{\text{ref}}$ is equal to $V_{\text{MPP}}$. At this point, the algorithm will stop operating and store the value unless any environmental changes are detected a change in $\Delta I$. The algorithm will re-calculate until

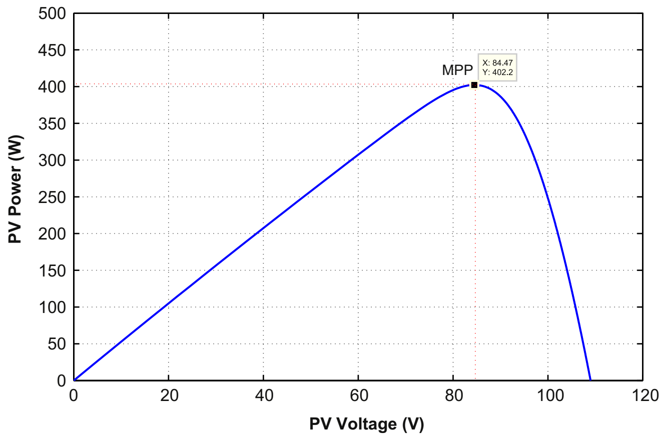


**Fig. 10.** The location of the true MPP under the *P–V* characteristic curve.

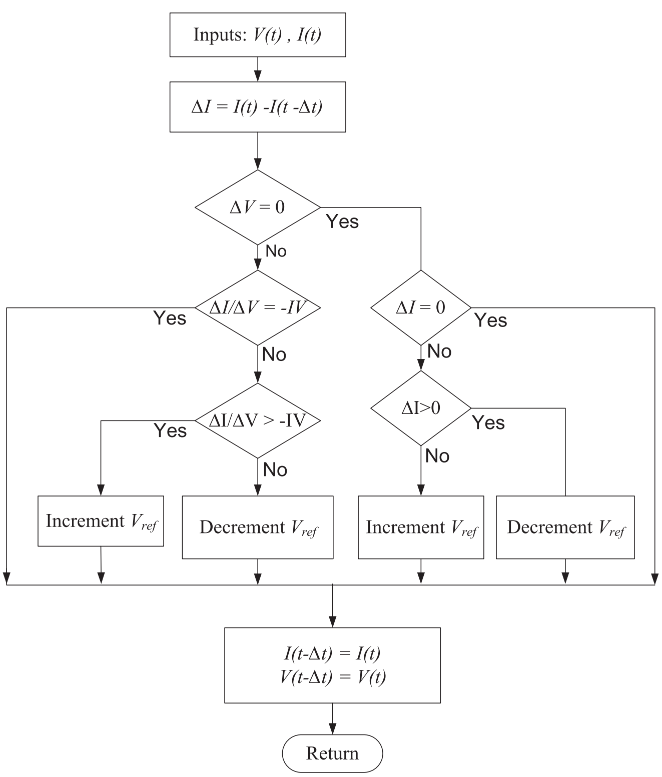


**Fig. 11.** The flow chart of incremental conductance MPPT algorithm.

optimum point is obtained [34]. The incremental size determines how fast the MPPT algorithm searches for the MPP. Large incremental size helps to reduce the duration of tracking process; however, the system will operate not only at the point of MPP but oscillate about this point [83].

The IncCond offers the advantage of better performance under rapidly varying atmospheric conditions as well as lower oscillation around MPP. However, the efficiency of IncCond to achieve MPP is about the same as the P&O method [79]. The drawback of this method is, under partial shading condition, it is not able to track the global MPP. Finally, the control circuitry of IncCond is complex which leads to a high system cost.

### 4.2. Hill climbing

The hill climbing (HC) algorithm is basically the same as the P&O, in that it regulates the PV voltage to follow the optimal setting point ($V_{MPP}$). The HC algorithm focuses on the perturbation of the duty-cycle of its power converter to find the MPP. The optimal point is continuously tracked and updated by the algorithm until the MPP, defined as $dP/dV=0$, is found. The current value of the *PV* power $P(k)$ is constantly compared to the previous calculated measurement, $P(k-1)$. If the value is the same, the controller will sense the *PV* voltage and *PV* current again; however, if the current power is greater than the previous value, the slope is complemented. The switching duty-cycle of the power converter keeps changing until the operating power oscillates at the MPP [27].

The HC algorithm provides an advantage in its simplicity of operation. The drawback of this method is that it fails to track the MPP under rapidly changing environmental conditions. Much research has been undertaken in order to improve the tracking performance of HC. For instance, Xiao and Dunford [30] introduced the modified adaptive hill climbing MPPT Method by including an automatic parameter to tune the system as well as control mode switching so that the algorithm can be applied under various environmental changes. Literature in [25] introduced a digital hill climbing method combined with a bidirectional current mode power cell for space application. The results show that the MPPT was a promising principle to gain maximum power from PV array. The flow chart of the hill climbing algorithm is shown in Fig. 12.

#### 4.2.1. Open-circuit voltage and short-circuit current

The open-circuit voltage, $V_{OC}$ [83] MPPT algorithm is a simplified technique in off-line (stand-alone) application. This method applies an approximately linear relationship between the open-circuit voltage and the maximum output voltage ($V_{MPP}$) of PV array under varying atmospheric conditions. This method can be approximated by

$$V_{MPP} \approx kV_{oc} \tag{14}$$

where $k$ is a constant that varies between 0.7 and 0.8 depending on the *PV* cell characteristic. Fundamentally, it is empirically measured based on the $V_{MPP}$ and $V_{OC}$ after determining the value of $k$ under changing atmospheric condition.

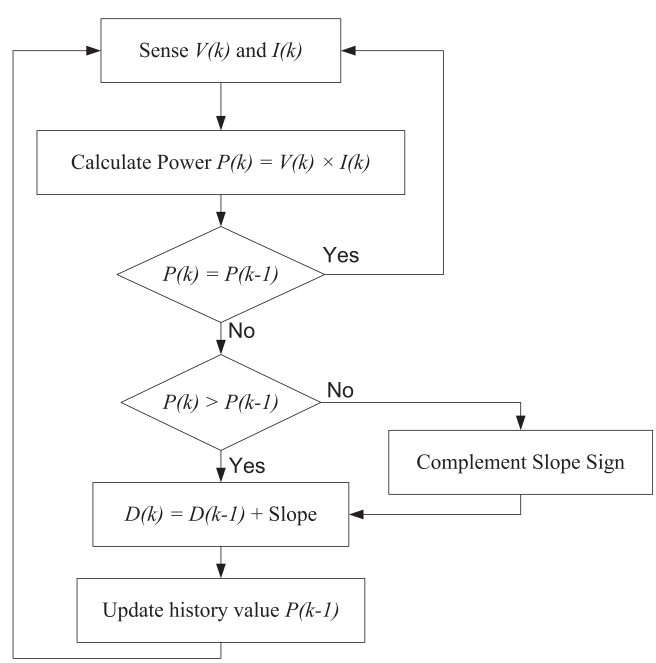


**Fig. 12.** The flow chart of Hill Climbing MPPT algorithm.

The $V_{OC}$ is measured by shedding the load of the PV array, allowing $V_{\text{MPP}}$ to be approximated. Although this MPPT is simple in the implementation, Eq. (14) is only an approximation, so the accuracy of the PV array operating at the MPP is not high. This is a disadvantage of this method, as well as the fact that the circuit operation might be interfered with by the periodic shedding of the load.

Another simplified off-line method is the short-circuit current technique, in which its operation is similar to the open-circuit voltage technique [83]. The approximately linear relationship between short-circuit current $I_{SC}$, and the current at maximum power point, $I_{\text{MPP}}$, is expressed by following equation:

$$I_{\text{MPP}} \approx kI_{SC} \tag{15}$$

where $k$ is a constant that is generally within the range of 0.8 to 0.9. Similar to the $V_{OC}$ method in measuring $I_{SC}$, load has to be shed. Then, $I_{\text{MPP}}$ can be determined. This method is much more accurate compare to $V_{OC}$ but it requires higher cost of implementation.

### 4.3. Ripple correlation current

Connecting the PV array to a DC–DC converter would create voltage ripple and current ripples due to the switching action of the converter. Therefore, the PV power produced would contain ripples which may affect the performance of the PV system. Refs. [43,44] reported on the ripple correlation control MPPT technique and its implementation. In order to reach the MPP, the power gradient must be zero. In order to achieve that, the RCC correlates between derivatives of the PV array power, varying $\dot{P}$ versus current, $i$ or voltage, $\tilde{V}$ which are both varying in time.

If either the PV current or voltage increases, the PV power also increases ($\dot{P}$ ÃÂ aA 0) in which the operating point always operates less than the MPP ($V < V_{\text{MPP}}$ or $i < I_{\text{MPP}}$). In contrast, when $V$ or $i$ increases but P decreases ($\dot{P} < 0$), the operating point is over the MPP ($V > V_{\text{MPP}}$ or $i > I_{\text{MPP}}$). Thus, combining these operations, $\dot{P}i$ or $\dot{P}\tilde{V}$ are positive on the left side of the MPP, zero at the MPP, and positive on the right side of the MPP. The voltage and current of the power converter can be increased or decreased depending on the type of power converter, thus the duty ratio can be controlled as:

$$d(t) = -k_3 \int \dot{P}\dot{V}\, dt \tag{16}$$

or

$$d(t) = k_3 \int \dot{P}i\, dt \tag{17}$$

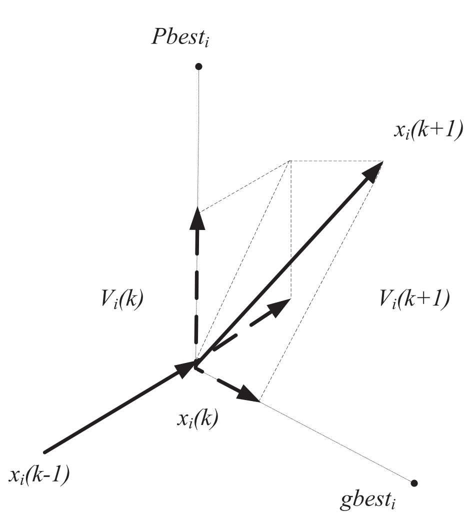


**Fig. 13.** An illustration of the particles movement in particle swarm optimization MPPT algorithm.

the RCC technique does not depend on the PV array parameters and it is able to track the correct MPP by controlling the duty-ratio of the power converter.

The RCC provides advantages of simple and less expensive analogue circuitry while quickly tracking the MPP in rapid environmental changes. Nevertheless, switching the frequency of the power converter limits the time taken by the controller to converge to the MPP [83]. Moreover, at low solar irradiance, this MPPT technique has the drawback of low tracking capability as it requires large tracking steps near the MPP.

### 4.4. Stochastic based MPPT algorithms

#### 4.4.1. Particle swarm optimization

The particle swarm optimization (PSO) is an algorithm that was proposed by J. Keneddy in 1995, which was inspired by the behavior of organisms such as a flock of birds and a shoal of fish. The concept of how they use their physical movement to adapt to the environment, by competition and cooperation, is adaptable for the optimization solution [57,84].

A number of particles move in a search space to find the best solution. The movement is adjusted by following the best found solution while trying out new solutions. To meet the optimal solution, the position of the particle has to follow the best position of the particle or the neighbour best position.

Position update and velocity update are the operators that govern the PSO, given by the following equations.

The velocity update is given by

$$V_i^{k+1} = wV_i^k + c_1 r_1 (pbest_i - x_i^k) + c_2 r_2 (gbest_i - x_i^k) \tag{18}$$

while the position update is expressed by

$$x_i^{k+1} = x_i^k + V_i^{k+1} \tag{19}$$

where,

$V_i^k$: current particle velocity, $V_i^{k+1}$: particle velocity update, $w$: inertia weight, $c_1$: influence of individual learning rate, $c_2$: influence of social learning rate, $pbest_i$: the best position found by the particle, $gbest_i$: the best solution found by the swarm, $c_1$ and $r_2$: two uniformly distributed random values to add randomness to particle movement, $x_i^k$: current particle position, $x_i^{k+1}$: particle position update.

The movement of particle to find optimal solution is given by Fig. 13 while the flow chart of the PSO is given in Fig. 14.

Assume that a PV array has an $N$ number of modules and is connected in series. Partial shading occurs on one of the PV modules. Thus, the voltage of a shaded PV module will be different from an unshaded module. Under this condition, multiple local maxima will occur on PV characteristic. The PSO MPPT reaches the optimal output when the global voltage is achieved.

In order to start the optimization, which is to find the global voltage in $P$–$V$ characteristic, the parameters of PSO need to be specified. These parameters include the variable dimensions that need to be optimized (voltage and power), swarm size and maximum iterations. The process is shown in Fig. 14. The global voltage $V_g$ with swarm size, NP can be defined as

$$x_i^k = V_g = [V_{g1,}\, V_{g2},\, V_{g3}, \ldots, V_{gj}] \\ j = 1, 2, 3, \ldots, \text{NP} \tag{20}$$

The best position (best value of power and voltage) that has PSO found so far is stored in $pbest$ and it keeps updating until achieving objective function.

$$pbest_i = x_i^k \tag{21}$$

The objective function is to find the maximum operating power in the system corresponding to its maximum voltage, which can

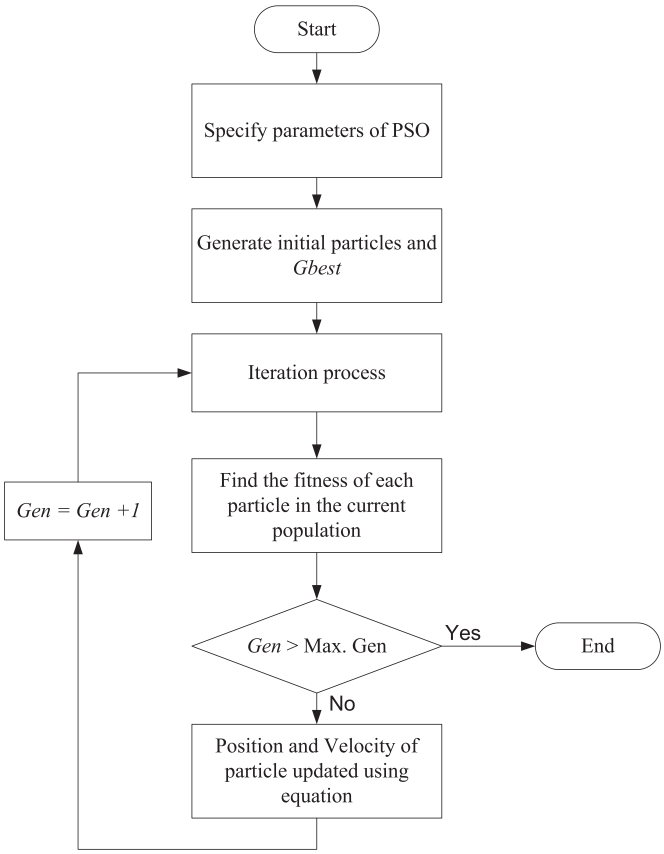


**Fig. 14.** The flow chart of particle swarm optimization for MPPT.

be defined as

$$f\,(x_i^k) > f\,(x_i^{k+1}) \tag{22}$$

where *f* function is the operating power of the PV array.

As partial shading causes the PV power changing, thus to find the optimum power, particles need to re-initialize to find the global maximum power point by the following condition:

$$\left|\frac{P(x_{i+1}) - P(x_i)}{P(x_i)}\right| > \Delta P \tag{23}$$

The re-initialization of each particle is significant in the PSO algorithm in order to identify each module that has the optimal terminal voltage [56]. Thus, the *pbest* and *gbest* can be updated automatically when there is a sudden change of solar irradiance or temperature. Therefore, the total output power of the PV system can be optimized. The PSO algorithm has been developed and modified by many researchers [56–60,85,86] in order to improve its tracking performance under partial shading condition. The MPPT controller based PSO algorithm was first introduced by [56] which proposed PSO algorithm for multiple PV arrays. This multidimensional search-based technique uses only one pair of sensors (voltage and current transducers). It is capable of detecting global maximum power point under partial shading conditions, where its reachability to global MPP is good. The author compared the performance of the PSO technique in tracking maximum power with the conventional hill climbing technique. The results showed that the PSO was able to track and measure PV energy 80% higher than the hill climbing with faster tracking time. The author [60] had improved the PSO algorithm for PV MPPT by adding another term in PSO algorithm. The term acts as repulsive force to the PSO agent to find the best voltage at any environmental changes. Thus, PSO MPPT is able to be more responsive to frequent change of solar irradiation. Comparing this to previous work, without adding the repulsive force, improvements on the PSO algorithm result in higher efficiency. By studying the characteristics of the PV in terms of voltage and power, authors in Ref. [85] had modified the conventional PSO. The author proposed modified particle swarm optimization for PV systems under extreme environmental condition. Maximum change in velocity had been restricted to a certain value determined by the study, while a random number of acceleration factors in conventional PSO equation had been removed. The performance of the proposed algorithm is compared with hill climbing algorithm, and the results show that the proposed algorithm has faster tracking speed and almost zero steady-state oscillation as compared with that of hill climbing algorithm. Overall, the study reveals that this algorithm is robust and fast in tracking the global MPP compared to the conventional method. Besides that, this algorithm works efficiently in searching the global peak under complex partial shading conditions.

### *4.4.2. Fuzzy logic controller*

The concept of fuzzy logic is based on applying expert knowledge in designing a fuzzy logic controller. It does not require any technical knowledge for the exact model, while its simplicity of the design gives it an advantage in tracking its maximum power point under varying atmospheric conditions. It deals with imprecision and information granularity in the form of linguistic constructs such as "many", "low", "medium", "often" and "few" [67].

The FLC consists of four stages; fuzzification, rule base, inference engine and defuzzification as shown in the FLC block diagram in Fig. 15. During the fuzzification stage, the membership function values are assigned into linguistic variables. The number of linguistic variables assigned is user-defined depending on the accuracy of the desired output. For the five fuzzy rule bases, linguistic variables can be Negative Big (NB), Negative Small (NS), Zero (Z), Positive Small (PS) and Positive Big (PB). Higher numbers of linguistic variables produce more stable and accurate results in the design [66]. However more precise results require a longer time to solve. The type of membership function can also be varied. They can use either trapezoidal, triangular or Gaussian but normally the triangular shape is used as shown in Fig. 16, while the range of membership functions, the parameter *a* and *b*, and the number of membership functions can be decided by previous knowledge of proposed scheme parameters [70]. Otherwise, it can be selected by trial and error method based on user knowledge provided that the input data can cover the appropriate region of interest [87].

From the diagrams, inputs of fuzzy are variable which are usually an error, $E$ and change in error, $\Delta E$. Calculation of error and change in error is flexible depending on the user, however, to have $dP/dV$ at MPP, the approximation can be defined as

$$E(x) = \frac{P(x) - P(x-1)}{V(x) - V(x-1)} \tag{24}$$

$$\Delta E(k) = E(k) - E(k-1) \tag{25}$$

where $x$ is the sampling time while $P(x)$ is the instantaneous power of the PV system and $V(x)$ gives the corresponding instantaneous voltage. The $E(x)$ value will show the location of the operating load power point whether on the left or right side of the MPP or at the point of the MPP. The $\Delta E(x)$ indicates the moving direction of the operating power point.

The inputs of $E$ and $\Delta E$ are then calculated and converted to linguistic variables which generate the output, $D$ from the look up rule base table, as in Table 2. Another advantage of using the FLC, is the gap for each operating point for the membership function can be adjusted in order to get the optimum MPPT. The membership

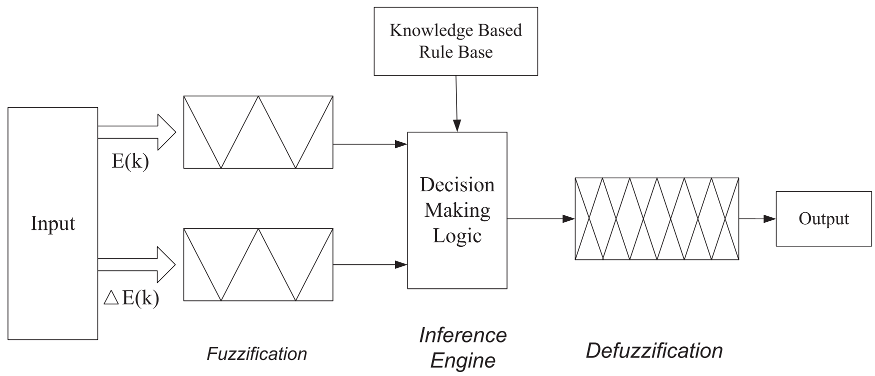


**Fig. 15.** The block diagram of fuzzy logic controller.

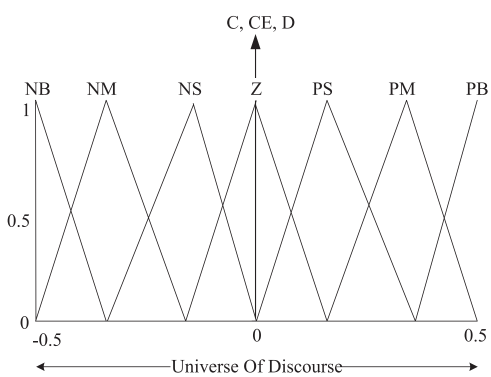


**Fig. 16.** The membership functions of fuzzy logic controller.

**Table 2**
Rule base table of fuzzy logic controller.

| **$\Delta E$** | ***E*** | | | | |
|---|---|---|---|---|---|
| | **NB** | **NS** | ***Z*** | **PS** | **PB** |
| **NB** | ZE | ZE | NB | NB | NB |
| **NS** | ZE | ZE | NS | NS | NS |
| ***Z*** | NS | ZE | ZE | ZE | PS |
| **PS** | PS | PS | PS | ZE | ZE |
| **PB** | PB | PB | PB | ZE | ZE |

function can be denser at the middle to get more precise output [68].

The fuzzy output is associated with the fuzzy input which is derived by the understanding of the system behaviour. This is done by the inference engine which applies rules from the rules base Table 1. It is noted that the rules base table requires user knowledge to form fuzzy rules and it can be expressed in the form of IF-THEN [29]. Mamdani's inference engine method is commonly used [69] which uses min–max operation in fuzzy operation. In Ref. [66], the diagonal zero line in the rule base table represents the switching line of acceleration and deceleration. Acceleration and deceleration represents environmental changes, either rapid changes or slow changes that affect the system.

In the defuzzification stage, the FLC output controller is converted back to numerical variables from linguistic variables by using the same membership function but with different ranges depending on user defined. The output of the FLC will provide a signal to control the duty-cycle of power converter in order to track the maximum output. As the defuzzification result, the output of the FLC will be able to maintain the operating voltage of the PV array to its maximum value under partial shading condition. Hence, energy conversion efficiency of the system can be improved.

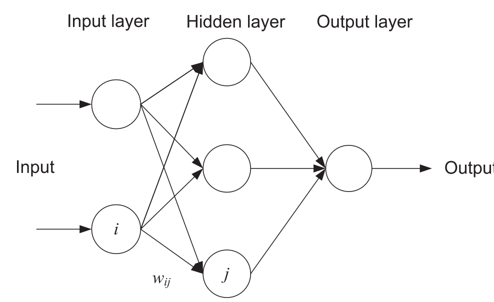


**Fig. 17.** The three layers of ANN structure [83].

Literature [88] has embedded fuzzy logic to the P&O technique to vary the size of perturbed voltage, $\Delta V$, so that the true MPP can be tracked and reached faster. Based on the research, when the PV array experienced 50% of shading, the operating voltage is able to shift to the point where power is optimum compare to the conventional P&O which traps at any local peaks.

### 4.4.3. *Artificial neural network*

The application of artificial neural network (ANN) in various fields has been increasing as it gives an advantage of performing on non-linear tasks. It is based on learning process and does not have to be reprogrammed. ANN consists of three layers; input layers, hidden layers and output layer. ANN is modelled as weights, which interconnect between neural networks and have their own strength. As shown in Fig. 17, the interconnection between $i$ and $j$ gives by $w_{ij}$. All inputs are summed together and modify by the weights.

It is noted that, the artificial neural network is a system with structure that receives an input, processes the data, and provides an output. The number of nodes and the parameters of ANN can be varied depending on designers. Input variables can be defined from inputs of PV array such as temperature, rate of solar irradiance and short-circuit current or open-circuit voltage. The output of the ANN can be used to drive a power converter by adjusting the duty-cycle signal or by having an input for another controller so that the PV system operates at or near to the MPP. The operation to gain accurate results depends on the algorithm performance in the hidden layers and the training process of the neural network [83].

In partially shaded condition, ANN is trained to predict the global MPP voltage and power by observing the $P$–$V$ curve under several shading condition on the PV array [66]. Then, the difference between the prediction voltage and the actual voltage from the PV array gives an error input for the MPPT controller to track the maximum power.

There are two topologies in the ANN connection, namely the feed-forward neural networks as shown in Fig. 18 and the recurrent neural networks as shown in Fig. 19. For feed-forward, the input–output data is strictly feed-forward [89]. The data processing can be extended to multiple layers with no feedback connections. The connection is directly from inputs of units to the outputs of units in the same layer or previous layers. By contrast, recurrent neural network depends on the dynamical properties of the network. The recurrent network contains feedback which embodies short term memory. The activation values will experience a relaxation process, in which the activations will not change when neural network turns to a stable state [90].

In order to enhance the MPPT for PV system under partial shading condition, the authors from Ref. [66] had proposed ANN combined fuzzy logic with polar information controller to find maximum power. Three layers feed-forward of ANN is trained under a number of partially shaded PV array to find the optimum PV voltage. The developed method had been compared to the P&O for several shading patterns in a certain period of time. The results show that the tracking efficiency of the developed method is twice higher than the P&O method.

### 4.4.4. *Differential evolution*

Differential evolution (DE) is an evolutionary algorithm that was introduced by Storn and Price in 1996 [91]. The DE is a family of Genetic Algorithm (GA) which is a stochastic based algorithm to find for optimization. Thus, the operations of the DE are likely to be the same as of the GA: initialization, mutation, crossover, evaluation and selection. Like other algorithms, the DE also has search variable vectors in a NP population.

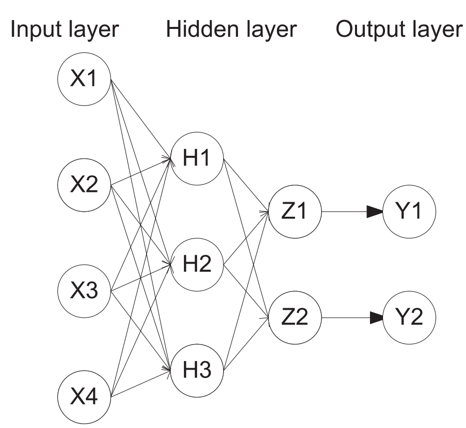


**Fig. 18.** Feed-forward neural network with four inputs and two outputs.

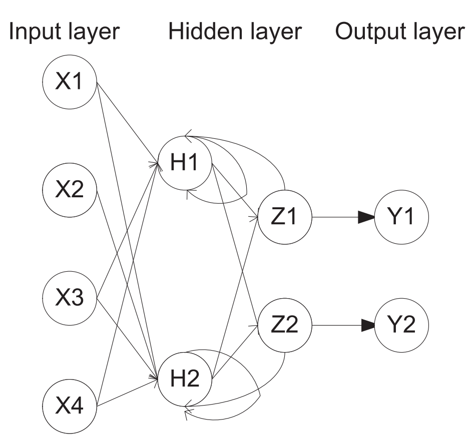


**Fig. 19.** Recurrent neural network with four inputs and two outputs.

### 4.4.5. *Initialization*

To start, the DE optimization is required to set the initial parameters, population and maximum generation. The initial vector is chosen randomly to cover the entire search space [91]. In order to obtain better search results, the parameter should lie within a certain range. Initially, $j$th parameter is formed after the DE algorithm is run. The parameter is initialized somewhere in the decided range which has a lower and upper limit, $x_j^L$ and $x_j^U$, respectively. Then, the $j$th parameter in $i$th population is

$$x_{i,j}(0) = x_j^L + rand\ (0,1).\ (x_j^U - x_j^L) \tag{26}$$

*rand* $(0, 1)$ is uniformly distributed random between 0 and 1.

### 4.4.6. *Mutation*

For each generation, individuals will become a target vector. Due to the mutation operation, each individual will be mutated to form a second individual called a mutant vector, $\overrightarrow{V}_i(t)$. To create $\overrightarrow{V}_i(t)$ for the $i$th population, three other parameter vectors, $r_1, r_2$ and $r_3$ are chosen randomly from the current population. A scalar number $F$, scales the difference of any two of the three vectors which will be added to the third one that is obtained from the mutant vector $\overrightarrow{V}_i(t)$. The process forms a new $j$th parameter in the population and can be expressed as

$$v_{i,j}(t+1) = x_{r1,j}(t) + F.(x_{r2,j}(t) - x_{r3,j}(t))\cdots \tag{27}$$

### 4.4.7. *Crossover*

In crossover operation, the parent will expand for next generation. By mixing the target vector with a mutant vector in crossover operation, third individual will produce a trial vector. The DE has two different crossover schemes, namely the exponential and the binomial schemes [92].

In exponential crossover, integer $n$ is chosen randomly among the numbers of $[0, D-1]$ which become a starting point of the target vector. Another integer, $L$ is also chosen from interval of $[1, D]$ to represent number of components. Choosing $n$ and $L$, trial vector:

$$\overrightarrow{u}_{i,j}\ (t) = [u_{i,1}\ (t), u_{i,2}(t), \ldots, u_{i,D}(t) \tag{28}$$

is formed with

$$\begin{aligned} u_{i,j}(t) &= v_{i,j}\ (t) \quad \text{for } j = \langle n \rangle D, \langle n+1 \rangle D, \ldots, \langle n-L+1 \rangle D \\ &= x_{i,j}\ (t) \end{aligned} \tag{29}$$

for

$$\begin{aligned} j &= \langle n \rangle D, \langle n+1 \rangle D, \ldots, \langle n-L+1 \rangle D \\ &= x_{i,j}(t) \end{aligned} \tag{30}$$

The angular bracket $\langle\ \rangle D$ denotes a modulo function with modulus $D$. Then, $(L > m) = (\mathrm{CR})^{m-1}$ for any $m > 0$. The CR is the crossover constant which control parameter of the DE.

In binomial crossover, the crossover is achieved on the $D$ variables whenever a randomly picked number between 0 and 1 is within the CR value. This scheme is given as

$$\begin{aligned} u_{i,j}(t) &= v_{i,\ j}(i) \quad \text{if } rand(0,1) < \mathrm{CR}, \\ &= x_{i,\ j}(t) \end{aligned}$$

else

### 4.4.8. *Evaluation and selection*

The population size is important to be kept constant over the subsequent generations; hence a selection operator will take action. In the selection operation, if the trial vector is able to find the best fitness value compared to the parent target vector, the trial vector will replace the parent for the next generation. Finding the best individual in a local search, the competition is one to one, while in the global search, it is necessary to find for the best

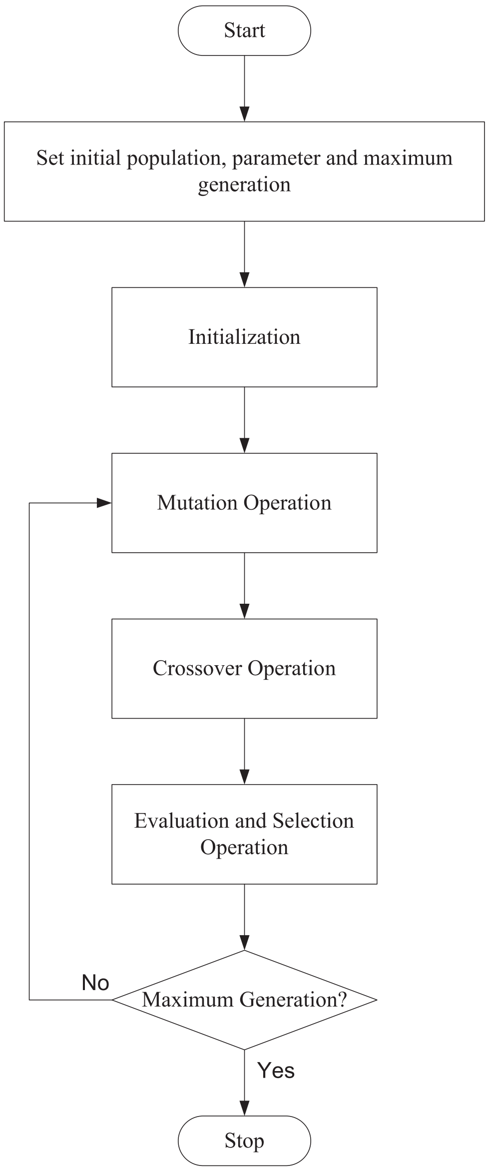


**Fig. 20.** The flow chart of differential evolution MPPT algorithm.

individual among the population. The flow chart as shown in Fig. 20 shows how the DE is conducted to find for optimum value.

The author [62] has introduced MPPT algorithm using DE for partial shading conditions. Comparing DE and the most common conventional MPPT algorithm, P&O, DE can converge very fast and reach the MPP without any oscillation even under partial shading conditions. Under rapidly changing environmental conditions, the DE is able to track to MPP while the P&O cannot reach to the global MPP.

## 5. Genetic algorithm

Ramaprabha [63] has introduced a MPPT controller using genetic algorithm (GA) for partial shading conditions. The principle of the GA is similar to the DE algorithm which is based on genetic and evolution biological behaviour. In the GA, it contains three basic operators which are the selection, crossover and mutation. In a random population, selected individual is represented as a candidate solution to the optimization. The mechanism of the GA in order to find optimization can be simplified as in Fig. 21.

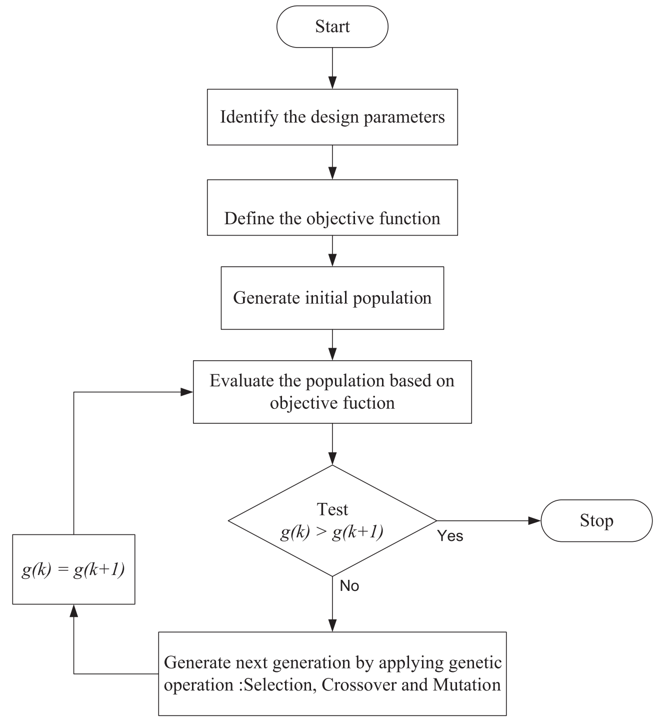


**Fig. 21.** The flow chart of genetic MPPT algorithm.

Based on Fig. 21, the GA parameters need to be identified. The parameters are constituted by genes in a chromosome. These can be either in the form of binary code or real code. Each of the chromosomes will present different parameters which mean that there is a possibility of variable solutions that can be obtained. The objective function gives a performance index of the GA to determine the performance of each chromosome. The objective function is formed based on the performance requirement of each problem such as convergence value and error.

Next, the initial population is generated by randomly picking a set of chromosomes. The population size is depending on the complexity of optimization problems. Fast convergence solutions with only a few generations is required if the population size is larger. However, a larger population size will take longer to track as the computation time is depending on the number of used generations. When the convergence value is satisfied, the operation will stop. Nevertheless, the operation will continue by applying genetic operations which are selection, crossover and mutation in order to generate the next generation. This process will continue until optimization is achieved.

In genetic operations, the algorithm is to be ensured that it will not stop searching at local maximum but the process will continue until the algorithm tracks the true global peak. In Ref. [87], a genetic algorithm is used to optimize the fuzzy logic controller for the maximum power point tracking under varying atmospheric conditions. By applying the GA, the FLC parameters such as rules base and membership function can be tuned to optimal value where the highest fitness in the last generation will determine the shape of membership function as well as rule base table. Thus, this will improve the performance of the FLC in the optimization process.

## 6. Discussions

There are many MPPT techniques that can be found from literature reviews. Techniques can range from conventional techniques to recent developed techniques which share the same aim in order to maximize the PV output power regardless of uniform irradiance or partial shading. The MPPT techniques can be categorized based on their characteristics. In this paper, the discussion is made into the following factors, namely the design complexity, ability to track the true MPP, cost consideration, sensitivity to the environmental change and also the convergence speed.

### 6.1. Design complexity

It is important to choose the most suitable MPPT based on its design complexity. The efficiency and complexity of MPPT depend on how accurate the algorithm has predicted by calculation, in searching for the true MPP or the local peaks. Otherwise, the optimum solar energy isn't harvested by the PV system. On the other hand, the implementation of the MPPT depends also on the user knowledge in handling the MPPT, in which, one may be good in dealing with analog circuits while others prefer digital circuits. Nevertheless, most of the stochastic based MPPT algorithms are implemented in digital form which requires software and computer programming.

### 6.2. Ability to track the true MPP

As the solar irradiance is unpredictable, there is a tendency that partial shading could occur. This condition would lead to the formation of multiple peaks on the *P–V* characteristic, which directly affects the tracking efficiency of the PV system. Conventional MPPT algorithms are not capable in tracking the true MPP while stochastic based MPPT algorithms are equipped with the capability to track the global peak over multiple local peaks. In this context, the PSO and the DE algorithms have the highest capability while the ANN and the FLC requires an additional driver to drive the controller to extract the maximum power from the system.

### 6.3. Cost consideration

In some applications especially commercialization, cost is the main factor to be considered. The cost of MPPT depends on the number of sensors implemented in the system, the complexity of the design as well as the choice of analog or digital system. The number and type of sensors implemented influence the system cost because in most cases, current sensors are much more pricy than voltage sensors. The types of hardware used to control the MPPT algorithm also affect the implementation cost while the choice of algorithm used determines the system capital cost. Besides that, analog circuits are lower in cost than digital circuits which require computer programming.

### 6.4. Sensitivity

A good MPPT algorithm must be sensitive enough to any atmospheric condition changes. The MPPT algorithm must be able to respond quickly and track the maximum power point of the particular PV system at the given condition, be it uniform solar irradiance or partially shaded condition. The PSO and the DE are among the MPPT algorithms that are able to automatically update the optimum power of the PV system when there is a change in solar irradiance and ambient temperature.

### 6.5. Convergence speed

A high sensitivity MPPT algorithm should be able to converge to the required operating voltage and current at a very high speed, regardless of a gradual or drastic change of environmental conditions. Comparatively, the conventional MPPT techniques takes a longer time to converge to the true MPP as compared to the stochastic techniques. In addition, the stochastic algorithms perform tracking at minimal or negligible oscillation. In short, in designing a PV system, one should take into the consideration the MPPT algorithm convergence speed as well as the tracking performance to avoid any loss of energy.

The abovementioned PV MPPT algorithms are summarized in both Tables 3 and 4, respectively.

## 7. Conclusion

This paper has comparatively reviewed the available MPPT algorithms for PV systems, ranging from the conventional techniques to the most recent developed stochastic based algorithms. The control strategy to extract the maximum power from PV array varies from one MPPT algorithm to another. The design criteria of MPPT algorithms can be categorized into the design complexity, ability to track the true MPP, cost consideration, sensitivity to the environmental change, the convergence speed and the efficiency of the controller to operate at the prevailing atmospheric condition. Based on the literature review, it can be concluded that the conventional MPPT algorithms work fine under uniform solar irradiance. However, these algorithms fail to drive the PV system operating point to the true MPP under rapidly changing atmospheric and partial shading conditions. This issue was overcome by using the new MPPT techniques based on stochastic and artificial intelligence, which showed good performance in tracking global peak. Moreover, the tracking process is faster and able to reach the true MPP or the global peak without oscillation. Today, research on MPPT algorithms is ongoing with the ultimate aim to find a simple, low cost and highly efficient algorithm. Almost all renewable energy comes with non-linear characteristic by nature; hence the MPPT controller is essential to ensure the system is operating at the optimum condition and to make best use of the expensive technology. Therefore, it is hoped that in the near future, the dependency on conventional fossil fuel resources can be further reduced when the output power from renewable resources can be fully harvested and utilized.

**Table 3**
The characteristics of conventional MPPT techniques [83].

| Criteria | P&O | HC | IncCond | $V_{oc}$ | $I_{sc}$ | RCC |
|---|---|---|---|---|---|---|
| PV array dependant | No | No | Yes | Yes | Yes | No |
| Convergence Speed | Varies | Varies | Varies | Medium | Medium | Fast |
| Periodic tuning | No | No | No | Yes | Yes | No |
| Sensed parameters | Voltage, current | Voltage, current | Voltage, current | Voltage | Current | Voltage, current |
| Complexity | Low | Low | Medium | Low | Medium | Low |
| Analog/digital | Both | Both | Digital | Both | Both | Analog |
| Ability to track true maxima | Yes | Yes | Yes | No | No | Yes |
| Sensitivity | Moderate | Moderate | Moderate | Low | Low | Moderate |

**Table 4**
The characteristics of MPPT techniques based on stochastic algorithm and artificial intelligence.

| Criteria | PSO | FLC | ANN | DE | GA |
|---|---|---|---|---|---|
| PV array dependant | No | No | No | No | No |
| Convergence speed | Fast | Moderate/low | Moderate/low | Fast | Fast |
| Periodic tuning | No | Yes | Yes | No | No |
| Voltage and/or current sensing | Yes | Yes | Yes | Yes | Yes |
| Complexity | Simple | Complex | Complex | Simple | Simple |
| Analog/digital | Digital | Digital | Digital | Digital | Digital |
| Ability to track true maxima | Yes | Poor tracking performance | Poor tracking performance | Yes | Yes |
| Initial parameter requirement | Yes | Yes | Yes | Yes | Yes |
| Sensitivity | High sensitivity | Moderate | Moderate | High sensitivity | Moderate |

## References


[1] R. 21. Renewables 2012 global status report, REN 21 renewable energy policy network for the 21st century; 2012.

[2] Ottmar Edenhofer RPM, Sokona Youba. Renewable energy sourced and climate change mitigation: special report of the intergovenrmental panel on climate change. Cambridge Unversity, Cambridge UK 2012.

[3] R. 21. REN 21 renewables 2013 global status report, REN 21 renewable energy policy network for the 21st century; 2013.

[4] Parida B, et al. A review of solar photovoltaic technologies. Renewable Sustainable Energy Rev 2011;15:1625–36.

[5] Baños R, et al. Optimization methods applied to renewable and sustainable energy: a review. Renewable Sustainable Energy Rev 2011;15:1753–66.

[6] Wasynczuk O. Dynamic behavior of a class of photovoltaic power systems. IEEE Power Eng Rev 1983;3:36–7.

[7] Hua CLin JR. DSP-based controller application in battery storage of photovoltaic system. In: Presented at the proceedings of the IEEE IECON 22nd international conference on industrial electronics, control, and instrumentation, 1996.

[8] Rahovich MASaLM. Maximum power point regulator for 4 kW solar cell array connected through invertor to the AC grid, 1996.

[9] Zhang AA-AaL. Optimal control of a grid-connected PV system for maximum power point tracking and unity power factor. In: Presented at the proceedings of the seventh international conference on power electron. variable speed drives, 1998.

[10] Kasa TIN, Iwamoto H. Maximum power point tracking with capacitor identifier for photovoltaic power system. Electr Power Appl 2000;147:497–502.

[11] Zhang AA-AL, Bai Y. Real-time maximum power point tracking for grid-connected photovoltaic systems. In: Proceedings of eighth international conference on power electronics and variable speed drives, pp. 124-129, 2000.

[12] Lin J-R, Hua C-C. Fully digital control of distributed photovoltaic power systems. In: Proceedings of the IEEE international symposium industrial electro, pp. 1-6, 2001.

[13] ChiangC-CHM-L, Lin J-R. Direct power control for distributed PV power system. In: Proc. power convers. conf, Osaka, pp. 311-315, 2002.

[14] Chomsuwan PPK, Monyakul V. Photovoltaic grid connected inverter using two-switch buck-boost converter. In: Presented at the conf. record 29th IEEE photovoltaic spec. conf, 2002.

[15] Chen Y-THaC-HC-H, Hsiao Y-T. Maximum power tracking for photovoltaic power system. In: Presented at the conf. record 37th IAS annual meeting industry application conference 2002.

[16] Jung GYY, Choi J, Choi J. High-frequency DC link inverter for grid-connected photovoltaic system. In: Presented at the conf. record 29th IEEE photovoltaic spec. conf, 2002.

[17] Agarwal SJ a V. A new algorithm for rapid tracking of approximate maximum power point in photovoltaic systems. IEEE Power Electron Lett 2004;2:16–9.

[18] Agbossou KTafticht T. Development of a MPPT method for photovoltaic systems. In: Presented at the Canadian conf on elect comput eng, Canada, 2004.

[19] Femia N, et al. Optimization of perturb and observe maximum power point tracking method. IEEE Trans Power Electron Jul. 2005;20:96–973.

[20] Tang PJWaL. A single cell maximum power point tracking converter without a current sensor for high performance vehicle solar arrays. In: Proceeding 36th annual IEEE power electronic specific conference, 165-171, 2005.

[21] D'Souza LACLNS, Liu X. An intelligent maximum power point tracker using peak current control. In: Proceeding of 36th annual IEEE power electronic specific conference, 172-177, 2005.

[22] Kasa TI N, Chen L. Flyback inverter controlled by sensorless current MPPT for photovoltaic power. IEEE Trans Ind Electron 2005;52:1145–52.

[23] Buciarelli BLGLL, Lyon EF, Rasmussen NE. The energy balance associated with the use of a MPPT in a 100 kW peak power system. In: Presented at the IEEE photovoltaic specific conference, 1980.

[24] Enslin JDvWaJHR. A study of wind power converter with microprocessor based power control utilizing an over synchronous electronic scherbius cascade. In: Proceedings IEEE international power electronic conference, pp. 766-777, 1983.

[25] Teulings WJA, et al. A new maximum power point tracking system. In: Proceeding 24th annu. IEEE power electron spec conf, pp. 833-838, 1993.

[26] Kim HJY, Kim D. A new peak power tracker for cost-effective photovoltaic power system. In: Presented at the proc of 31st intersociety energy convers eng conf, 1996.

[27] Shimizu TH, Kimura O, G. A novel high performance utility interactive photovoltaic inverter system. IEEE Trans Power Electron 2003;18:704–11.

[28] Koutroulis E, et al. Development of a microcontroller-based, photovoltaic maximum power point tracking control system,. IEEE Trans Power Electron 2001;16:46–54.

[29] Veerachary TS M, Uezato K. Maximum power point tracking control of IDB converter supplied PV system. Electr Power Appl 2001;148:494–502.

[30] Xiao W, Dunford WG. A modified adaptive hill climbing MPPT method for photovoltaic power systems. In: Presented at the proc of 35th annu IEEE power electron spec conf, 2004.

[31] Boehringer AF. Self-adapting dc converter for solar spacecraft power supply. IEEE Trans Aerosp Electron Syst 1968;4:102–11.

[32] Lindena ENCaS. Comparison of candidate solar array maximum power utilization approaches. In: Presented at the intersociety energy conversion eng conference, 1976.

[33] Zhao JH a G. Controlled power-interface between solar cells and ac sources. IEEE Trans Power Electron 1989;8:654–62.

[34] Hussein KH, Mota I. Maximum photovoltaic power tracking: an algorithm for rapidly changing atmospheric conditions. IEE Proc Gener Transm Distrib 1995;142:59–64.

[35] Brambilla MGA, Garutti A, Ronchi F. New approach to photovoltaic arrays maximum power point tracking. In: Presented at the proc 30th annu IEEE power electron spec conf, 1999.

[36] Irisawa TSK, Takano I,, Sawada Y. Maximum power point tracking control of photovoltaic generation system under non-uniform insolation by means of monitoring cells. In: Presented at the conf. record 28th IEEE photovoltaic spec conf, 2000.

[37] Kim H-GAT-Y, Park SK, Lee Y-K. A novel maximum power point tracking control for photovoltaic power system under rapidly changing solar radiation. In: IEEE int symp Ind electron, pp. 1011-1014, 2001.

[38] Kuo T-JL Y-C, Chen J-F. Novel maximum-power-point tracking controller for photovoltaic energy conversion system. IEEE Trans Ind Electron 2001;48:594–601.

[39] Yu YSJGJ, Choi JY, Choy I, Song JH, Kim GS. A novel two-mode MPPT control algorithm based on comparative study of existing algorithms. In: Presented at the conf record 29th IEEE photovoltaic spec conf, 2002.

[40] Kobayashi KT, Takano I, Sawada Y. A study on a two stage maximum power point tracking control of a photovoltaic system under partially shaded insolation conditions. In: Presented at the power engineering society general meeting, 2003.

[41] Wu NPW, Qiu W, Rustom K, Kasparis T, Batarseh I. DSP-based multiple peak power tracking for expandable power system. In: Presented at the 18th annu IEEE appl power electron conf expo, 2003.

[42] Midya PTKP, Turnbull RJ, Reppa R, Kimball J. Dynamic maximum power point tracker for photovoltaic applications. In: Presented at the proc 27th annu IEEE power electron spec conf, 1996.

[43] Esram T, et al. Dynamic maximum power point tracking of photovoltaic arrays using ripple correlation control. IEEE Trans Power Electron 2006;21:1281–91.

[44] Casadei D, et al. Single- phase single- stage photovoltaic generation system based on a ripple correlation control maximum power point tracking. IEEE Trans Energy Convers 2006;21:562–8.

[45] Beukes BBaHJ. Finding an optimal PV panel maximum power point tracking method. In: Proc 7th AFRICON conf. Africa, pp. 1125-1129, 2004.

[46] Noguchi STT, Nakamoto R. Short-current pulse based adaptive maximum-power-point tracking for photovoltaic power generation system. In: Proc. 2000 IEEE int symp Ind electron, pp. 157-162, 2000.

[47] Mutoh TMN, Okada K, Sakai M. Prediction-data-based maximum-power-point-tracking method for photovoltaic power generation systems. In: Proc. 33rd annu. IEEE power electron. spec. conf, pp. 1489-1494, 2002.

[48] Xu SYaS. Photo-voltaic power converter with a simple maximum-power-point-tracker. In: Presented at the proc. 2003 int. symp. circuits system, 1982.

[49] vanWyk JJSaJD. A simplified maximal power controller for terrestrial photovoltaic panel arrays. In: Proc. 13th annu. IEEE power electron. spec. conf, 361-367, 1982.
[50] Buresch. M. Photovoltaic Energy Syst 1983.
[51] Hart HM BG W, Cox CH. Experimental tests of open loop maximum-power-point tracking techniques. Solar Cells 1984;13:185–95.
[52] Patterson DJ. Electrical system design for a solar powered vehicle. In: Presented at the Proc. 21st annu. IEEE power electron. spec. conf, 1990.
[53] Masoum HD MA S, Fuchs EF. Theoretical and experimental analyses of photovoltaic systems with voltage and current-based maximum power-point tracking. IEEE Trans Energy Convers 2002;14:514–22.
[54] Noh D-YLH-J, Hyun D-S. An improved MPPT converter with current compensation method for small scaled PV-applications. In: Proc. 28th annu conf Ind electron soc, pp. 1113-1118, 2002.
[55] Kobayashi HMK, Sekine Y. A novel optimum operating point tracker of the solar cell power supply system. In: Proc. 35th annu. IEEE power electron. spec. conf, pp. 2147-2151, 2004.
[56] Miyatake M, et al. Maximum power point tracking of multiple photovoltaic arrays: a PSO approach. IEEE Trans Aerosp Electron Syst 2011;27:367–80.
[57] Zainuddin NANN, et al. Optimizing filter parameters using Particle Swarm Optimization. In: Presented at the signal 64 processing and its applications (CSPA), 2010 6th international colloquiun, 2011.
[58] Ishaque K, et al. Maximum power point tracking for PV system under partial shading condition via particle swarm optimization . In: Presented at the applied power electronics colloquium (IAPEC), 2011 IEEE; 2011.
[59] Ngan MS, Tan CW. Review of the maximum power point tracking for stand alone photovoltaic systems. Sol Energy Mater Sol Cells 2006;90:1555–78.
[60] Phimmasone TEV, Kondo Y, Miyatake M. Improvement of the maximum power point tracker for photovoltaic generators with particle swarm optimization technique by adding repulsive force among agents. In: Presented at the electrical machines and systems international conference, 2009.
[61] Rad MR RMR, Abbas S, Akbari S. A maximum power point tracking for photovoltaic arrays using particle swarm optimization techniques plus fuzzy cognitive networks. Adv Electr Eng Syst 2012;1:54–60.
[62] Ishaque K, et al. A novel maximum power point tracking control of photovoltaic system under partial and rapidly fluctuating shadow conditions using differential evolution. In: Presented at the 2010 IEEE symposium on industrial electronics and applications, 2010.
[63] Ramaprabha R, Mathur BL. Genetic algorithm based maximum power point tracking for partially shaded solar photovoltaic array. Int J Res Rev Inf Sci (IJRRIS) 2012;2:161–3.
[64] Syafaruddin TH, Karatepe E. Investigation of ANN perforance for tracking the optimum points of PV module under partially shaded conditions. In: IPEC conference proceedings, pp. 1186-1191, 2010.
[65] Vincenzo D. Artificial neural network for real time modelling of photovoltaic system under partial shading. In: Presented at the sustainable energy technologies IEEE international conference, 2010.
[66] Syafaruddin, et al. Artificial neural network-polar coordinated fuzzy controller based maximum power point tracking control under partially shaded conditions. IET Renew Power Gener 2009;3:239–53.
[67] Sivanandam SN, et al. Introduction to fuzzy logic using MATLAB. Heidelberg New York: Springer; 2007; 430 (editor).
[68] Veerachary TS M, Uezato K. Fedforward maximum power point tracking of PV systems using fuzzy controller. IEEE Trans Aerosp Electron Syst 2002;38: 969–81.
[69] Balasubramanian G, Singaravelu S. Fuzzy logic controller for the maximum power point tracking in photovoltaic system. Int J Comput Appl 2012;41:22–8.
[70] Islam MA, et al. Maximum power point tracking of photovoltaic arrays in matlab using fuzzy logic controller. In: Presented at the India conference (INDICON), 2010.
[71] Kang JSKSJ, Choi JS, Jang MG, Mun JH. A novel MPPT control of photovoltaic system using FLC algorithm. In: Presented at the 11th international conference on control, automation and systems, 2011.
[72] Ait Cheikh e a MS. Maximum power point tracking using fuzzy logic controller scheme. J Renewable Energies 2007;10:387–95.
[73] Takun SKaCJP. Maximum power point tracking using fuzzy logic control for photovoltaic systems. In: Proceedings of the international multiconference of engineers and computer scientists, 2011.
[74] Rodrigues EMG, et al. Simulation of a solar cell considering single diode equivalent circuit model. In: Presented at the international conference on renewable energies and power.
[75] ⟨http://ecee.colorado.edu/~ecen2060/matlab.html⟩. (2008). Introduction to power electronics course notes, ECEN 2060.
[76] Liang TH, et al. Development of generalized photovoltaic model using MATLAB/Simulink. In: Presented at the proceeding of the world congress on engineering and computer science, 2008.
[77] Chan DSH, Phang JCH. Analytical methods for the extraction of solar-cell single- and double-diode model parameters from *I–V* characteristics. IEEE Trans Electron Devices 1987;34:286–93.
[78] Ishaque K, et al. Simple, fast and accurate two diode model for photovoltaic modules. Sol Energy Mater Sol Cells 2011;95:586–94.
[79] Salas EO V, Barrado A, Lazaro A. Review of the maximum power point tracking for stand alone photovoltaic systems. IEEE Trans Energy Convers 2006;22: 439–49.
[80] Onat N. Recent developments in maximum power point tracking technologies for photovoltaic systems. Int J Photoenergy 2010:1–10.
[81] Huang TL, et al. Maximum power point tracking for photovoltaic power system. Tamkang J Sci Eng 2005;8:147–53.
[82] Hohm DP, Ropp ME. Comparative study of maximum power point tracking algorithms. Prog Photovoltaics Res Appl 2003;11:47–62.
[83] Esram T, Chapman PL. Comparison of photovoltaic array maximum power point tracking techniques. IEEE Trans Energy Convers 2007;22.
[84] Eberhart JKR. A new optimizer using particle swarm theory. In: Presented at the micro machine and human science proceedings of the sixth international symposium, 1995.
[85] Ishaque ZS K. A deterministic particle swarm optimization maximum power point tracker for photovoltaic system under partial shading condition. IEEE Trans Ind Electron 2013;60:3195–206.
[86] Kuei- Hsiang Chao L-Y C, Liu Hsueh-Chien. Maximum power point tracking method based on modiifed particle swarm optimization for photovoltaic systems. Int J Photoenergy 2013;2013:1–6.
[87] Messai A, et al. Maximum power point tracking using GA optimize fuzzy logic controller and its FPGA implementation. Solar Energy 2011;86:265–77.
[88] Ji Y-H, et al. A real maximum power point tracking method for mismatching compensation in PV array under partially shaded conditions. IEEE Trans Power Electron 2011;26:1001–9.
[89] Al-kazemi B, Mohan CK. Training feed-forward neural networks using multi-phase particle swarm optimization. In: Presented at the Neural Information Processing. ICONIP. vol 02, 2002.
[90] Pearlmutter BA. Dynamic recurrent neural networks 1990, http://www.cim.mcgill.ca/~yon/ai/readings/pearlmutter90dynamic.pdf.
[91] Storn R, Price K. Differential evolution—a simple and efficient heuristic for global optimization over continuous spaces. J Global Optim 1997;11:341–59.
[92] Das S, et al. Particle swarm optimization and differential evolution algorithms: technical analysis, applications and hybridization perspectives. In: Advances of computational intelligence in industrial systems. 116, (ed), 2008.